Excitation of Chirping Whistler Waves in a Laboratory Plasma

B. Van Compernolle, X. An, J. Bortnik, R. M. Thorne, P. Pribyl, and W. Gekelman

Phys. Rev. Lett. **114**, 245002 — Published 17 June 2015

DOI: 10.1103/PhysRevLett.114.245002

Excitation of chirping whistler waves in a laboratory plasma

B. Van Compernolle,[1,*] X. An,[2] J. Bortnik,[2] R. M. Thorne,[2] P. Pribyl,[1] and W. Gekelman[1]

[1] *Department of Physics, University of California, Los Angeles*
[2] *Department of Atmospheric and Oceanic Sciences, University of California, Los Angeles*

(Dated: May 20, 2015)

Whistler mode chorus emissions with a characteristic frequency chirp are important magnetospheric waves, responsible for the acceleration of outer radiation belt electrons to relativistic energies and also for the scattering loss of these electrons into the atmosphere. Here, we report on the first laboratory experiment where whistler waves exhibiting fast frequency chirping have been artificially produced using a beam of energetic electrons launched into a cold plasma. Frequency chirps are only observed for a narrow range of plasma and beam parameters, and show a strong dependence on beam density, plasma density and magnetic field gradient. Broadband whistler waves similar to magnetospheric hiss are also observed, and the parameter ranges for each emission are quantified.

Whistler mode chorus waves are excited in the low density plasma region outside of the Earth's plasmasphere following the convective injection of low-energy ($\sim$ 10 keV) plasma sheet electrons into the inner magnetosphere during periods of enhanced geomagnetic activity [1, 2]. These waves are typically found in two distinct frequency bands with a gap near one half the electron cyclotron frequency [3]. They typically exhibit discrete rising or falling tones thought to originate from non-linear processes [4], but can also occur as wide-band incoherent hiss [5]. These chorus waves play a critical role in the acceleration of low-energy trapped radiation belt electrons to relativistic energies, and can also lead to rapid scattering loss into the atmosphere [6–9].

Extensive theoretical work has been done in the past but none adequately describe the features of discrete, chirping chorus waves. For instance, linear theory [10] predicts the regions in the frequency domain that are unstable to wave growth, but cannot predict the saturation amplitude of the wave, nor the discreteness or frequency chirp rate. Extensive numerical simulations have been performed [4, 11, 12] under fairly restrictive assumptions that reproduce some of the features of chirping chorus waves, and certain scaling laws have been developed as a result, but these laws require extensive testing against observations to ascertain their validity. Such experimental testing is difficult to perform in space, since spacecraft do not generally have access to the source distribution of electrons that originally generated the waves, but can be readily performed in a laboratory setting, which is the motivation of the present study. Similarly, previous attempts to remotely excite artificial whistler waves have been made in the Earth's near-space environment and have yielded interesting results [13, 14], but have been difficult to probe and control.

This Letter reports the first experiment where chorus-like whistler waves, i.e., discrete whistler waves exhibiting rapid frequency chirping have been artificially excited in a laboratory plasma. Energetic electrons emitted from a beam source are launched into a cold plasma and generate both broadband hiss-like whistler waves and discrete chorus-like whistler waves for specific beam and plasma parameters. Fast frequency chirping has been observed before in laboratory settings, for the Alfvén wave range of frequencies in experiments with energetic ion beams [15–17].

The experiment is performed on the upgraded Large Plasma Device (LAPD) [18, 19] at the Basic Plasma Science Facility (BaPSF) at UCLA. The LAPD is a long cylindrical device, with axial magnetic field and a 18 m long 60 cm diameter quiescent plasma column (1 Hz repetition rate, Helium fill gas at $3{\cdot}10^{-5}$ Torr, $T_e \leq 0.5$ eV). A range of plasma parameters were explored for this study, listed in Table I. Typical absolute values in the laboratory are quite different from those found in the magnetosphere but the dominant scaled dimensionless quantities are similar.

A 10 cm diameter electron beam source (0.5 kV $\leq V_{beam} \leq$ 4 kV) [23, 24] is introduced into the machine (Fig. 1) opposite the LAPD plasma source. The beam source is angled to 45 degrees with respect to the magnetic field in order to provide sufficient free energy in the electron distribution for the cyclotron growth of whistler waves. The magnitude of the field at the beam source is restricted to low values, in the range of $\sim$ 50 G, in order to allow accelerated electrons to escape the tilted

	LAPD	Inner Magnetosphere
n_0 (cm^{-3})	$5 \cdot 10^8$ - $5 \cdot 10^{10}$	1 - 10^3
B_0 (G)	20 - 60	$5 \cdot 10^{-4}$ - 10^{-1}
ω_{pe}/Ω_e	1 - 12	2 - 15
n_b/n_0	0.001 - 0.04	10^{-4} - 1
$\tilde{B}/B_0$	$10^{-5} - 10^{-4}$	$10^{-5} - 10^{-3}$
β_e	$10^{-6} - 10^{-4}$	$10^{-5} - 10^{-3}$

TABLE I. Plasma parameters in the laboratory and in the magnetosphere, plasma density [20], magnetic field strength, ratio of plasma frequency to cyclotron frequency [21], ratio of beam density to plasma density [22], ratio of whistler wave amplitude to background magnetic field strength [21, 22], ratio of electron thermal pressure to magnetic pressure.

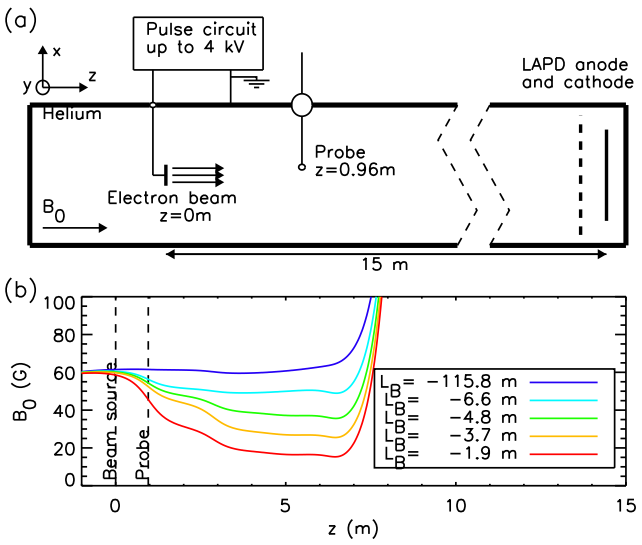

FIG. 1. (a) Schematic of the experimental setup, not to scale. A 10 cm diameter electron beam launches electrons with energies up to 4 keV. Probes measure plasma parameters and detect wave activity. (b) Magnetic field profiles used in the experiment and magnetic field gradient scale lengths L_B at the location of the probe.

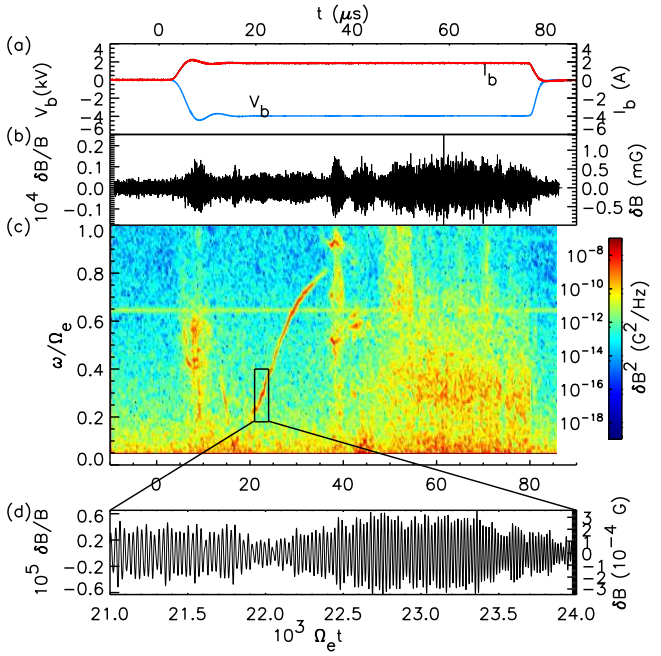

FIG. 2. (a) Time series of beam source voltage (blue) and total beam current (red) emitted by the LaB_6 disk. (b) Time series of fluctuations in the transverse magnetic field normalized to the local background field. (c) Spectrogram of the time series, showing a clear rising tone in the first half, followed by hiss-like broadband wave activity in the second half. (d) Zoom-in on the first part of the rising tone clearly shows the frequency increasing with time.

beam source assembly. Figure 1(b) shows the magnetic field profiles adopted in the experiment, along with the magnetic field gradient scale length L_B at the location of the probe, i.e., the inverse of $\frac{1}{B_0}\frac{dB_0}{dz}$. The magnetic field at the LAPD plasma source is 350 G, which is the minimum field required for reliable plasma production. Measurements of plasma parameters and wave activity were taken in the 7 m long low field region between the beam source and the transition to the high field region. The start of the electron beam pulse is taken as $t = 0$ and the location of the electron beam source as $z = 0$.

Figure 2 shows an example of beam generated wave activity for a 4 keV beam firing into a cold plasma with $\omega_{pe}/\Omega_e = 3$ and $n_b/n_0 = 0.015$. Time series of the total beam current and the applied beam voltage are shown in panel (a). After an initial overshoot both the voltage and current reach a constant level within 10 microseconds. The accompanying time series of perpendicular magnetic field fluctuations in panel (b) demonstrate the increase in wave activity during the time when the electron beam is present. The beam spontaneously excites electromagnetic waves in the whistler wave frequency range, i.e. with frequencies $\Omega_i < \omega < \Omega_e$, as well as near electron cyclotron frequency harmonics. The latter has been observed before in dedicated experiments [25] and is attributed to the finite Larmor orbit of the electron beam. The data in Fig. 2(b) is low pass filtered below Ω_e since the focus of this paper is on the whistler wave frequency range.

The time series in Fig. 2(b) is visualized using a dynamic spectrogram displayed in Fig. 2(c), which shows a whistler-mode discrete rising tone in the first half of the pulse, similar to chorus. The frequency sweep rate of the rising tone $\frac{df}{dt}$ is on the order of 7 MHz/μs, or in dimensionless units $\frac{d(\omega/\Omega_e)}{d(\Omega_e t)} \simeq 4 \cdot 10^{-5}$. For comparison, typical frequency sweep rates in the magnetosphere are in the range of $\frac{d(\omega/\Omega_e)}{d(\Omega_e t)} \simeq 10^{-5} - 10^{-4}$ [26–29]. Fig. 2(d) clearly illustrates the increase in frequency in the time domain during a portion of the rising tone.

To verify the identity of these waves, polarization parameters for these discrete tones were obtained following the methodology of *Means* [30, 31]. For the discrete tone in Fig. 2 the analysis shows that this is a right handed whistler wave with high polarization ratio of more than 95%. The wave normal angle is roughly 30°. The broadband emissions are more field aligned.

The last 30 μs of the beam pulse in Fig. 2(c) show enhanced wave activity in a broad band between 0.2 Ω_e and 0.5 Ω_e. The wave intensity is similar in amplitude to the rising tone and is reminiscent of hiss emissions found in the magnetosphere [5]. In certain cases the hiss-like and chorus-like features can occur during the same beam pulse as in Fig. 2(c), but they generally do not occur at the same time, i.e., when a discrete tone is present it suppresses any other emission. The wave activity at other frequencies outside of the discrete tone remains at

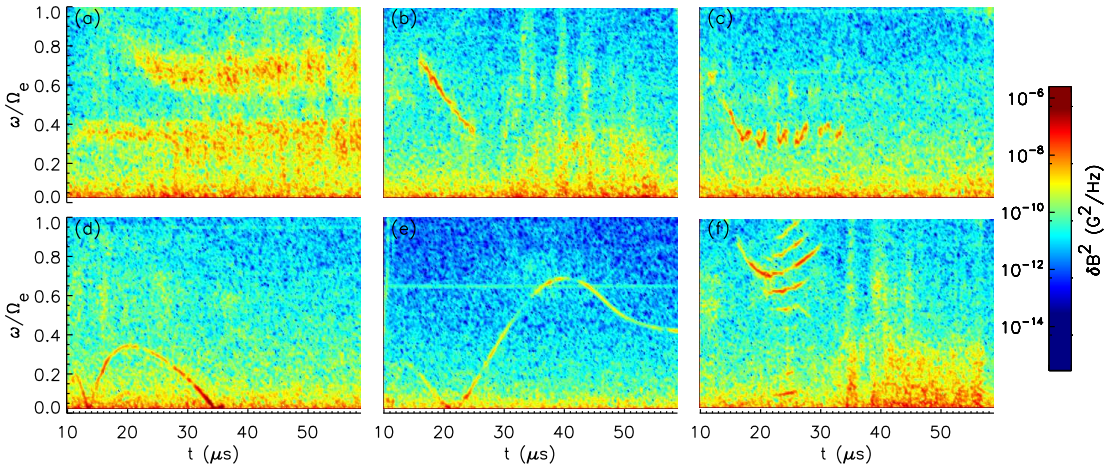

FIG. 3. Spectrograms of additional types of beam generated wave emissions, ranging from hiss-like, falling tones, multiple consecutive chirps, hooks and chirping at multiple frequencies. Plasma and beam parameters for (a)-(f) respectively: ω_{pe}/Ω_e = 11.2, 2.8, 3.6, 2.8, 2.8, 2.8; n_b/n_0 (%) = 0.1, 1.6, 1.0, 1.5, 0.8, 1.6. The beam source voltage is 3 kV for all cases. Audification of each of these cases is available online.

values close to the natural plasma noise level which is present before the beam pulse starts. This indicates that the fast electron distribution is significantly modified by the excitation of the rising tone such that the broadband hiss-like features are suppressed.

Apart from rising tones such as those illustrated in Fig. 2(c) a rich variety of beam-generated wave activity is observed in the whistler range. Figure 3 shows a representative selection ranging from (a) hiss-like emissions in a lower band below $\Omega_e/2$ and an upper band above $\Omega_e/2$, (b) falling tone followed by broadband activity below $\Omega_e/2$, (c) multiple consecutive short chirps, (d) double hook chirp emanating from the pre-existing low frequency wave activity, (e) long extended rising/falling chirp crossing the $\Omega_e/2$ mark, and (f) multiple simultaneous chirps at different frequencies followed by broadband wave activity below $\Omega_e/2$. For all these cases the beam source voltage is 3 kV. The relevant plasma and beam parameters are listed in the caption of Fig. 3. The magnetic field profile for these cases is plotted in Fig. 1(b) with $L_B = -4.8$ m, except for panel (b) and (f) which were obtained at a nearly uniform 60 G field.

The relative occurrence rates of broadband hiss-like emissions and frequency chirping chorus-like emissions were investigated as a function of beam density, plasma density and magnetic field gradient scale length. Data is taken in a radial line at $z = 0.96$ m through the region with strongest wave activity. A plasma shot with at least one discrete frequency chirp is counted as a discrete event. Broadband wave activity an order of magnitude above the noise is counted as a broadband event. A single plasma shot can have both discrete and broadband events.

A scan of beam density was done at $\omega_{pe}/\Omega_e = 3.2$ in a magnetic field profile with L_B = -4.8 m (Fig. 1(b)). Fig. 4(a) shows that no wave activity above the noise is detected at low beam densities. As the beam density is increased discrete whistlers are first observed. There is a clear optimum beam density for excitation of discrete chirping waves; curiously, chirping whistler waves are not seen at the highest beam densities either. Broadband waves are mostly seen for larger density ratios, $n_b/n_0 >$ 1%, at this ratio of $\omega_{pe}/\Omega_e = 3.2$. Similar trends were observed for chorus and hiss in space [22].

A second parameter scan shown in Fig. 4(b) is performed by varying the plasma density at fixed beam density, and with fixed magnetic field profile the same as above. This changes both the ratio of ω_{pe}/Ω_e and the ratio of n_b/n_0. Frequency chirping occurs in a narrow range of $\omega_{pe}/\Omega_e \simeq 2$ - 4, similar to space observations [5]. It is not clear if the absence of chirping waves at larger ω_{pe}/Ω_e is due to the increasing density or due to the decreasing ratio n_b/n_0 as in Fig. 4(a) since these vary simultaneously. It is not possible to keep n_b/n_0 fixed throughout this n_0 scan because the beam source cannot deliver enough beam current at the higher plasma densities. Broadband waves occur both at low values of ω_{pe}/Ω_e (high values of n_b/n_0 as in Fig. 4(a)), and at large $\omega_{pe}/\Omega_e > 4$, similar to hiss emissions found in the magnetosphere [5]. Higher plasma densities favor the excitation of broadband emissions which is evident from their excitation even at low beam densities, and from the lower threshold for broadband waves at large n_b/n_0, i.e., $n_b/n_0 > 1$ % at $\omega_{pe}/\Omega_e = 3.2$ (Fig. 4(a)) compared to $n_b/n_0 > 3$ % at $\omega_{pe}/\Omega_e < 2$ (Fig. 4(b)). The broadband waves generated at lower beam densities occur in a narrower frequency band, typically $\Delta\omega/\Omega_e < 0.1$, whereas at the higher beam densities $\Delta\omega/\Omega_e > 0.2$ is routinely seen.

A third scan, displayed in Fig. 4(c), was done at

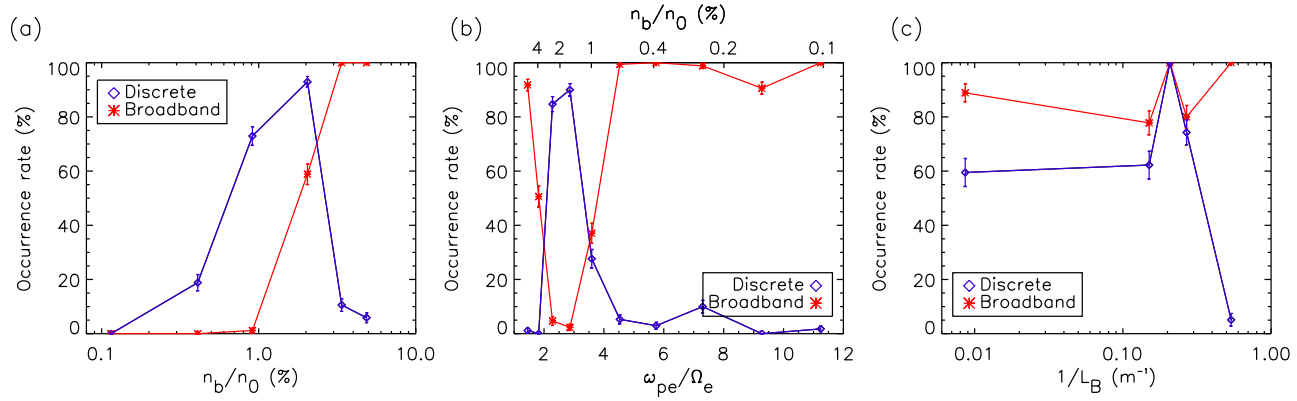

FIG. 4. Occurrence rates for discrete and broadband emissions (a) versus beam density at fixed plasma density, (b) versus plasma density at fixed beam density and (c) versus magnetic field gradient at fixed plasma density and fixed beam density.

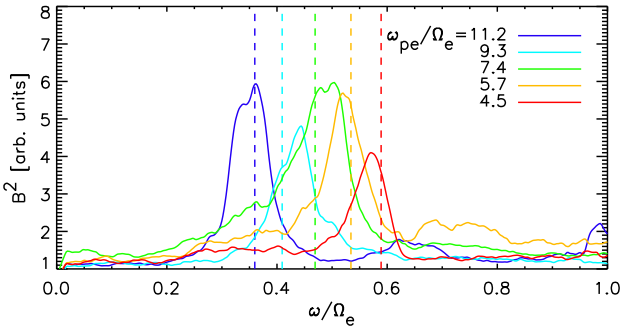

FIG. 5. Measured power spectra at different values of ω_{pe}/Ω_e, with linear theory predictions for the excited frequency indicated by the dashed lines.

$\omega_{pe}/\Omega_e = 3.2$ by varying the magnetic field profile, as shown in Fig. 1(b). Steep magnetic field gradients dramatically suppress chirping whistler waves. At gentler gradients a clear optimum is reached for the occurrence of chirping waves; even for nearly uniform fields a relatively high occurrence rate is observed. Broadband emissions are relatively insensitive to the magnetic field gradient. The observed variation is thought to be due to the ratio of $n_b/n_0 \simeq 1.6\%$ being near the threshold value for the occurrence of broadband emissions, see Fig. 4(a).

The broadband emissions at $\omega_{pe}/\Omega_e > 4$ in Fig. 4(b) are well described by linear theory. The measured power spectra, plotted in Fig. 5, demonstrate the upshift in frequency as the plasma density is lowered. The observed frequency shift agrees well with predictions based on linear excitation through the Doppler shifted cyclotron resonance, i.e., by solving $\omega - k_\parallel v_{beam,\parallel} = \Omega_e$ and the whistler wave dispersion relation simultaneously. The normalized linear growth rate γ/Ω_e [32] for parallel propagating whistler waves is fairly insensitive to ω_{pe}/Ω_e at fixed n_b which may explain why broadband emissions are observed at the higher densities even though the density ratio n_b/n_0 decreases. Similarly the absence of hiss in Fig. 4(a) at low n_b/n_0 can be understood from linear growth rate estimates, given the dependence on the density ratio $(n_b/n_0)^\alpha$ ($\alpha = 1/3$ for a beam, $\alpha = 1$ for a bi-Maxwellian plasma). We should note that, although we launched a gyrating beam into the background plasma, the electron distribution function is redistributed to have a long tail up to the beam energy by other processes [23, 33–35].

The parametric behavior of the chirping whistler waves shows several similarities with the Omura model [11, 36]. The model conjectures that the interplay between trapped and untrapped electron populations in the presence of a gentle gradient in the background field leads to the formation of an electron phase space hole. This gives rise to a nonlinear resonant current which causes wave growth and frequency chirping. This is prohibited if a large background field gradient exists, which may explain the measured suppression of frequency chirps at large field gradients. The model predicts the existence of an optimum wave amplitude for the amplification of chorus waves, of which the measured optimum beam density in Fig. 4(a) may be evidence. Initial estimates of the predicted sweeping rate are an order of magnitude lower than observed, but may be due to the oblique nature of the observed discrete whistlers whereas the model assumes parallel propagation.

In this Letter, we have summarized results from the first laboratory experiment to observe whistler waves exhibiting fast frequency chirping, a phenomenon which has been observed in space for decades known as chorus waves. Broadband wave activity reminiscent to magnetospheric hiss is also observed. The occurrence rates have strong dependencies on fundamental parameters such as driving electron beam density, plasma density and magnetic field profile. The experiment allows, for the first time, to test under controlled conditions the leading hypotheses and identify missing elements in our current understanding of nonlinear whistler wave excitation.

The authors wish to thank G. J. Morales and T. A. Carter for insightful discussions. The research was

funded by the Department of Energy and the National Science Foundation by grant DE-SC0010578, which was awarded to UCLA through the NSF/DOE Plasma Partnership program. Work was done at the Basic Plasma Science Facility (BAPSF) also funded by DOE/NSF.

* bvcomper@physics.ucla.edu

[1] B. T. Tsurutani and E. J. Smith, Journal of Geophysical Research **79**, 118 (1974).

[2] O. Santolík, D. A. Gurnett, J. S. Pickett, M. Parrot, and N. Cornilleau-Wehrlin, Journal of Geophysical Research: Space Physics **108**, 1278 (2003).

[3] W. J. Burtis and R. A. Helliwell, Journal of Geophysical Research **74**, 3002 (1969).

[4] Y. Katoh and Y. Omura, Geophysical Research Letters **34**, L03102 (2007).

[5] W. Li, R. M. Thorne, J. Bortnik, X. Tao, and V. Angelopoulos, Geophysical Research Letters **39**, L18106 (2012).

[6] R. M. Thorne, W. Li, B. Ni, Q. Ma, J. Bortnik, L. Chen, D. N. Baker, H. E. Spence, G. D. Reeves, M. G. Henderson, C. A. Kletzing, W. S. Kurth, G. B. Hospodarsky, J. B. Blake, J. F. Fennell, S. G. Claudepierre, and S. G. Kanekal, Nature **504**, 411 (2013).

[7] G. D. Reeves, H. E. Spence, M. G. Henderson, S. K. Morley, R. H. W. Friedel, H. O. Funsten, D. N. Baker, S. G. Kanekal, J. B. Blake, J. F. Fennel, S. G. Claudepierre, R. M. Thorne, D. L. Turner, C. A. Kletzing, W. S. Kurth, B. A. Larsen, and J. T. Niehof, Science **341**, 991 (2013).

[8] R. M. Thorne, Geophysical Research Letters **37**, L22107 (2010).

[9] C. Cattell, J. R. Wygant, K. Goetz, K. Kersten, P. J. Kellogg, T. von Rosenvinge, S. D. Bale, I. Roth, M. Temerin, M. K. Hudson, R. A. Mewaldt, M. Wiedenbeck, M. Maksimovic, R. Ergun, M. Acuna, and C. T. Russell, Geophysical Research Letters **35**, L01105 (2008).

[10] C. Kennel, Physics of Fluids **9**, 2190 (1966).

[11] Y. Omura, Y. Katoh, and D. Summers, Journal of Geophysical Research: Space Physics **113**, A04223 (2008).

[12] Y. Omura, M. Hikishima, Y. Katoh, D. Summers, and S. Yagitani, Journal of Geophysical Research: Space Physics **114**, A07217 (2009).

[13] R. A. Helliwell, Radio Science **18**, 801 (1983).

[14] M. Golkowski, M. B. Cohen, D. L. Carpenter, and U. S. Inan, Journal of Geophysical Research: Space Physics **116**, A04208 (2011).

[15] K. McGuire, R. Goldston, M. Bell, M. Bitter, K. Bol, K. Brau, D. Buchenauer, T. Crowley, S. Davis, F. Dylla, H. Eubank, H. Fishman, R. Fonck, B. Grek, R. Grimm, R. Hawryluk, H. Hsuan, R. Hulse, R. Izzo, R. Kaita, S. Kaye, H. Kugel, D. Johnson, J. Manickam, D. Manos, D. Mansfield, E. Mazzucato, R. McCann, D. McCune, D. Monticello, R. Motley, D. Mueller, K. Oasa, M. Okabayashi, K. Owens, W. Park, M. Reusch, N. Sauthoff, G. Schmidt, S. Sesnic, J. Strachan, C. Surko, R. Slusher, H. Takahashi, F. Tenney, P. Thomas, H. Towner, J. Valley, and R. White, Phys. Rev. Lett. **50**, 891 (1983).

[16] M. Nave, D. Campbell, E. Joffrin, F. Marcus, G. Sadler, P. Smeulders, and K. Thomsen, Nuclear Fusion **31**, 697 (1991).

[17] W. W. Heidbrink, Plasma Physics and Controlled Fusion **37**, 937 (1995).

[18] W. Gekelman, H. Pfister, Z. Lucky, J. Bamber, D. Leneman, and J. Maggs, Rev. Sci. Instrum. **62**, 2875 (1991).

[19] D. Leneman, W. Gekelman, and J. Maggs, Rev. Sci. Instrum. **77**, 015108 (2006).

[20] B. Sheeley, M. Moldwin, H. Rassoul, and R. Anderson, Journal of Geophysical Research: Space Physics **106**, 25631 (2001).

[21] W. Li, R. M. Thorne, Y. Nishimura, J. Bortnik, V. Angelopoulos, J. P. McFadden, D. E. Larson, J. W. Bonnell, O. Le Contel, A. Roux, and U. Auster, Journal of Geophysical Research: Space Physics **115**, A00F11 (2010).

[22] X. Gao, W. Li, R. M. Thorne, J. Bortnik, V. Angelopoulos, Q. Lu, X. Tao, and S. Wang, Geophysical Research Letters **41**, 4805 (2014).

[23] B. Van Compernolle, J. Bortnik, P. Pribyl, W. Gekelman, M. Nakamoto, X. Tao, and R. M. Thorne, Phys. Rev. Lett. **112**, 145006 (2014).

[24] B. Van Compernolle, W. Gekelman, P. Pribyl, and C. Cooper, Phys. Plasmas **18**, 123501 (2011).

[25] R. L. Stenzel and G. Golubyatnikov, Physics of Fluids B **5**, 3789 (1993).

[26] E. Macúšová, O. Santolík, P. Decreau, A. G. Demekhov, D. Nunn, D. A. Gurnett, J. S. Pickett, E. E. Titova, B. V. Kozelov, J.-L. Rauch, and J.-G. Trotignon, Journal of Geophysical Research: Space Physics **115**, A12257 (2010).

[27] E. Titova, B. Kozelov, J. Smilauer, A. Demekhov, V. Y. Trakhtengerts, *et al.*, in *Annales Geophysicae*, Vol. 21 (2003) pp. 1073–1081.

[28] C. M. Cully, V. Angelopoulos, U. Auster, J. Bonnell, and O. Le Contel, Geophysical Research Letters **38**, L01106 (2011).

[29] X. Tao, W. Li, J. Bortnik, R. Thorne, and V. Angelopoulos, Geophysical Research Letters **39**, L08106 (2012).

[30] J. D. Means, Journal of Geophysical Research **77**, 5551 (1972).

[31] J. Bortnik, J. W. Cutler, C. Dunson, and T. E. Bleier, Journal of Geophysical Research: Space Physics **112**, A04204 (2007).

[32] T. F. Bell and O. Buneman, Phys. Rev. **133**, A1300 (1964).

[33] A. A. Ivanov and L. I. Rudakov, Soviet Physics JETP **24**, 1027 (1966).

[34] S. Kainer, J. Dawson, R. Shanny, and T. Coffey, Phys. Fluids **15**, 493 (1972).

[35] B. Lefebvre, L.-J. Chen, W. Gekelman, P. Kintner, J. Pickett, P. Pribyl, and S. Vincena, Nonlinear Processes in Geophysics **18**, 41 (2011).

[36] Y. Omura and D. Nunn, Journal of Geophysical Research: Space Physics **116**, A05205 (2011).